CrystEngComm

Accepted Manuscript

ROYAL SOCIETY OF CHEMISTRY

www.rsc.org/crystengcomm

From Discovery to Scale-up: α-Lipoic Acid:Nicotinamide Co-crystals in a Continuous Oscillatory Baffled Crystalliser

Lihua Zhao,[†] Vishal Raval,[†] Naomi E. B. Briggs,[†] Rajni M. Bhardwaj,[‡] Thomas McGlone,[†] Iain D. H. Oswald[‡], and Alastair J. Florence [†*]

[†]EPSRC Centre for Innovative Manufacturing in Continuous Manufacturing and Crystallisation c/o Strathclyde Institute of Pharmacy and Biomedical Sciences, University of Strathclyde, 161 Cathedral Street, Glasgow, G4 0RE, U.K.

[‡]Strathclyde Institute of Pharmacy and Biomedical Sciences, University of Strathclyde, 161 Cathedral Street, G4 0RE, U.K.

KEYWORDS: α-lipoic acid, co-crystals, nicotinamide, scale-up, continuous crystallisation, oscillatory baffled crystalliser, phase diagram

ABSTRACT: The crystalline nutritional supplement α-lipoic acid degrades rapidly on exposure to temperatures above its melting point 65 °C and to light. A small-scale experimental co-crystal screen has produced three novel co-crystals of α-lipoic acid that each display enhanced thermal stability and differences in aqueous solubilities compared to α-lipoic acid. In each case, the initial screening procedure produced tens of milligrams of material enabling initial identification, characterisation and crystal structure determination. The structure of the α-lipoic acid:nicotinamide co-crystal was determined by single crystal X-ray diffraction and used for subsequent phase identification. Scale-up of the co-crystallisation process of α-lipoic acid with nicotinamide was then investigated in a continuous oscillatory baffled crystalliser. Over 1 kg of solid co-crystals was produced using a continuous crystallisation process in a continuous oscillatory baffled crystalliser at a throughput of 350 g/hr yielding a purity of 99 % demonstrating this as an effective route to rapid scale-up of a novel co-crystal system.

*To whom correspondence should be addressed. E-mail: alastair.florence@strath.ac.uk. Telephone:+44-141-548-4877. Fax: +44-141- 552-2562.

INTRODUCTION

α-Lipoic acid (ALA; 1,2-dithiolane-3-pentanoic acid, Fig. 1) is an anti-oxidant and essential co-enzyme[1] used as a nutritional supplement with applications in the treatment of diabetic neuropathy[2, 3], Alzheimer's disease[4], metal poisoning[5, 6] and liver disease.[7] The molecule is prone to polymerisation and photo-decomposition associated with cleavage of the disulfide bond in the 1,2-dithiolane ring[8, 9] (Fig. 1). The crystal structure of ALA is known[10] (CSD[11]: THOCAR01) and various alternative crystalline forms with improved chemical stability have been reported including trometamol[12], carnitine[13], sodium and potassium salts.[14, 15] Improved stability of ALA has also been achieved by formulation of ALA with different components including polymers[16] and β-cyclodextrin.[17]

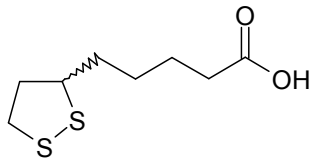

Fig. 1 Chemical structure of α-Lipoic acid (ALA)

Co-crystals[18-21] offer a route to engineer critical physico-chemical properties of specialty chemicals including pharmaceuticals[19, 22, 23] neutraceuticals[24, 25], energetic materials[26, 27] and agrochemicals.[28] Novel co-crystal forms also offer an opportunity to secure new intellectual property as part of the lifecycle management of chemical entities.[29] There are a number of examples of systems where co-crystals have been shown to improve the chemical stability of otherwise labile compounds.[30, 31] Co-crystallisation has also been used as an effective method to purify compounds during their industrial scale production.[32-34] Approaches to the effective selection of co-crystal formers for specific molecules have been widely reported.[21, 22, 35-38] Methods include identifying complementary hydrogen bonding

motifs[21, 37-39] and comparing the relative thermodynamic stabilities of the co-crystal and the component solid forms.[40]

Many different techniques have been described in the literature for obtaining co-crystal forms including solution crystallisation[41, 42], slow solvent evaporation[43, 44], slurry conversion[45], neat[46, 47] and liquid assisted grinding[48] as well as growth from melts.[49] Recently, the use of twin-screw extrusion for the preparation of pharmaceutical co-crystals has also been reported.[50-52] Among these methods, slow evaporation and grinding are convenient and efficient ways to produce milligram or gram quantities of novel co-crystals and are widely used for preparation.[53] Once new materials have been discovered and the evaluation of relevant physicochemical properties has informed the selection of the most promising forms for a particular application, it is of considerable interest to identify efficient and rapid means of scaling-up these novel crystalline forms to allow further testing or exploitation of the new materials at larger scales. Although the twin screw extruder method provides a good alternative for making co-crystals with scale-up potential, speed and solvent free conditions, it does have limitations. For example, it can only be applied to systems with pure components, cannot be used for purification purposes, and it is not suitable for thermally unstable chemicals such as ALA as elevated temperature is required for the formation of pure co-crystals.[50, 51] Achieving scale-up of co-crystal production remains a major challenge and there have been a small number of studies describing approaches for scale-up from gram to kilogram scales (Table 1).

Table 1 Reported studies on co-crystallisation scale-up

Co-crystal system	Scale	Method	Features	Ref
Carbamazepine (CBZ) :nicotinamide (NIC) and	1 L vessel	Solution cooling crystallisation	Through understanding phase diagrams	53
CBZ:saccharin	30 g	Solution cooling crystallisation	Based on the solubility of CBZ	54
Caffeine:Glutaric Acid	0.2 mol/kg caffeine in 1 L vessel	Solution cooling crystallisation	Using ATR-FTIR to monitor concentration	55
Caffeine:oxalic acid and AMG517:sorbic acid	200 g	Co-rotating twin screw extruder (16 mm)	Pre-mix two solid components; temperature 75 °C and 115 °C for two co-crystals	50
Ibuprofen:NIC	0.2 kg/hr	Co-rotating twin screw extruder (16 mm)	Premix two solid components, temperature 70-90 °C	51
API 1:benzoic acid and API :maleic acid	2.0 g (API)	Solution cooling crystallisation	Anti-solvent addition to achieve the supersaturation required for co-crystallisation	56
SAR1:benzoic acid	10 kg	Solution crystallisation	Using co-crystals for purification	33
Lamivudine intermediate co-crystal with (*S*)-(-)-BINOL	30 kg	Solution crystallisation	Separation of enantiomers by selective formation of the co-crystal with (*S*)-(-)-BINOL	34

Solution cooling crystallisation is one of the most widely used large scale manufacturing processes in the chemical and pharmaceutical industries providing effective purification and control of solid form and other particle attributes.[57] Mass and heat transfer are key process parameters controlling concentration and temperature gradients that can impact on local supersaturation and consequently crystal form, morphology, purity and particle size distribution[57] during cooling and anti-solvent crystallisation. These factors become more critical in co-crystallisation processes due to the need to control precisely the process path through multiple solid-liquid equilibria.

Continuous reaction, work-up and crystallisation are key operations in the drive towards improving manufacture in the chemical and pharmaceutical industries.[58-61] Continuous processing offers many potential advantages over traditional batch processes including consistent product quality, lower cost, small foot print, better process control, more efficient use of reagents, solvents, energy and space whilst minimising the production of waste materials and reactor downtime for reactor maintenance and cleaning. Whilst there remain challenges in the operation of continuous processing equipment within the highly regulated pharmaceutical manufacturing environment, there are significant drives to accelerate more widespread adoption of these technologies.[59, 62] The continuous oscillatory baffled crystalliser (COBC) has been reported to offer advantages in controlling crystallisation processes due to plug-flow mixing characteristics and rapid heat transfer properties.[63] The COBC is a tubular device containing periodically spaced orifice baffles with oscillatory motion superimposed on the net flow[64-69] (Fig. 2). Mixing in a COBC is provided by the generation and cessation of eddies when the flow interacts with the baffles and is governed by the oscillatory Reynolds number (Re_o) and the Strouhal number (St) which are normally used to characterise the oscillation intensity applied to the system.[64, 65, 70] The oscillatory Reynolds number and the Strouhal number are defined as:

$$Re_o = \frac{\pi f \chi_o \rho D}{\mu}$$

$$St = \frac{D}{4\pi\chi_o}$$

where D = column diameter (m), χ_o= centre-to-peak amplitude (m), f = frequency (Hz), ρ = density (kg m $^{-3}$) and μ = fluid viscosity (kg m^{-1}s^{-1}).

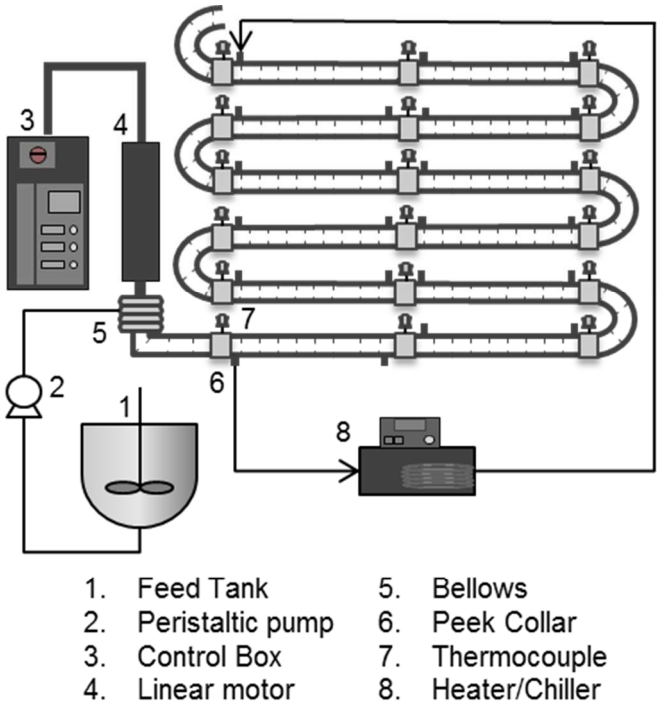

Fig. 2. A schematic diagram of a continuous oscillatory baffled crystalliser (COBC).

A batch OBC can be used to evaluate specific process conditions and linear scale-up from batch OBC to COBC has been described[63, 65, 71-73] where applying the same dimensionless numbers between systems ensures that hydrodynamic similarity remains consistent provided the geometric similarity is kept constant. Excellent heat transfer properties are achieved due to the high specific area per volume compared with a stirred tank reactor which can be particularly beneficial in providing precise control over cooling crystallisations.

In this study, the discovery and characterisation of three novel ALA co-crystals which are more stable than ALA is presented along with an assessment of the feasibility of scaling-up the co-crystallisation process of ALA with nicotinamide (NIC) from tens of mg to kg scale in a COBC. This is the first report of the scale-up for a continuous co-crystallisation process in a COBC.

EXPERIMENTAL SECTION

Materials. Nicotinamde (NIC), isonicotinamide (ISN), trans-cinnamamide, nicotinic acid, benzoic acid, benzamide, saccharin, urea and all solvents of analytical grade were purchased from *Sigma-Aldrich* and used as received. ALA (racemic) was purchased from *Molekula.* This contained small amounts of polymer and therefore was further purified by recrystallisation from a mixture of ethyl acetate-hexane (1:4) before co-crystallisation trials. In general, ALA was dissolved in ethyl acetate using ultrasound and the hexane was added with stirring. The total ALA:solvent ratio was 1:10 w/w. The mixture was filtered using vacuum to remove the insoluble polymer impurity and then slowly cooled to 5 °C. The pure solid was collected by filtration. Water used throughout the study was ultrapure provided from a *Thermoscientic Barnstead RO* water purification unit.

Methods.

X-Ray Crystallography. X-ray powder diffraction (XRPD) data was collected from a sample in a rotating 0.7 mm borosilicate glass capillary on a *Bruker AXS D8-Advance* transmission diffractometer equipped with θ/θ geometry, primary monochromated radiation (Cu Kα_1, λ = 1.54056 Å in the range 4 – 40° 2θ with a 0.016° 2θ step size and 5 or 8 s step^{-1} count time at room temperature (RT).

Single crystal diffraction data (SXD) were collected on a *Bruker Apex II* diffractometer with a charge coupled device (CCD) detector and graphite monochromated Mo Kα_1 radiation (λ = 0.71073 Å) with temperature control from an *Oxford Cryosystems Cryostream* device operating at -150 °C. Diffraction data were processed (cell refinement and data reduction) using *Bruker SAINT* and *APEX2* software[74], and structure solution and refinement were carried out by direct methods using SHELXS97 and SHELXL[75] respectively, accessed through the program package *WinGX*.[76]

Infrared Spectroscopy. Infrared (IR) spectra were obtained on a *Nicolet S10 Smart* ATR FT-IR spectrometer using *OMNIC* program (version 8.1). Solid samples were directly analysed without the

need for any prior sample preparation, and the data was collected within a range of 600-4000 cm^{-1} at RT.

Thermal Analysis. Differential scanning calorimetry (DSC) and thermogravimetric (TG) data were collected simultaneously on a *NETZSCH STA 449C* Instrument under nitrogen atmosphere using *NETZSCH* software. Samples were placed in a 25 μL aluminium crucible and analysed at a heating rate of 10 $^{\circ}C\ min^{-1}$. To determine thermal stability samples were heated at 10 $^{\circ}C\ min^{-1}$ to a temperature until the samples were completely melted; then the melt was subsequently cooled quickly to -50 $^{\circ}C$, and heated again at 10 $^{\circ}C\ min^{-1}$ to 300 $^{\circ}C$.

Stability by HPLC. The material was dried for 35 minutes and dissolved in isopropanol before filtering through a 0.45 μm syringe filter. Quantification was carried out by a *Varian Prostar* HPLC system using a standard calibration curve. HPLC column: *Waters Spherisorb ODS2*, 5 μm, 4.6 x 250 mm. Mobile phase: 500: 300: 200 (v/v, pH 2.8 buffer solution: acetonitrile: methanol). A UV detector was used at 330 nm.

Preparation of Co-crystals by Liquid-assisted Grinding. Equimolar amounts of ALA and co-crystal former (1:1 molar ratio) to a total weight of *ca*. 100 mg and a drop of ethanol were mixed and placed in the ball mill chamber of a *Retsch MM400* mixer mill. The sample was milled at 25 Hz for 5 minutes.

Preparation of Co-crystals by Solution Crystallisation. Saturated solutions of ALA and selected co-formers were prepared individually in appropriate solvents at RT and mixed in a 10 mL vial. Half of the solution was left at -10 °C and the other half of the solution was left at RT for slow evaporation. Solids formed were filtered and analysed by XRPD, DSC and FT-IR. Eight co-formers were used in the trials including NIC, ISN, nicotinic acid, benzoic acid, benzamide, trans-cinnamamide, saccharin, urea (chemical structures are provided in the ESI).

Polymorph Screen of ALA:NIC Co-crystals. A single crystal of ALA:NIC co-crystal was grown from the saturated solution of ALA:NIC in 1:1 v/v mixture of IPA:hexane by isothermal solvent evaporation at RT. An extensive polymorph screen was carried out using a variety of crystallisation methods

including solvent evaporation in pure and co-solvent systems at RT, cooling crystallisation, vapour diffusion and liquid diffusion. Various solvent systems were screened for crystallisation including methanol, ethanol, isopropanol (IPA), 1-butanol, 1-octanol, cyclohexanol, acetone, acetonitrile, hexane, 1:1 IPA:hexane, dichloromethane, tetrahydrofuran, 1,4-dioxane, ethyl acetate, butyl acetate, diethyl ether, diisopropyl ether, t-butyl methyl ether, cyclohexane, cyclopentane, toluene, water, dichloromethane, nitromethane, formamide, 1,2-dimethoxyethane, 1:1 IPA:diisopropyl ether, 1:1 ethanol:diisopropyl ether, diethyl carbonate and IPA:water. The resulting solids were analysed by XRPD.

Solubility Measurement of ALA:NIC Co-crystals. Solubility of ALA, NIC and 1:1 ALA:NIC in 1:1 IPA:hexane was measured in an *Avantium Crystalline* with built-in cameras for visualisation. Co-crystal samples with different concentrations were prepared and dissolution and nucleation temperatures were determined using turbidity and imaging method. Heating and cooling rates of 0.5 ^{o}C min^{-1} were applied, and a magnetic stirring bar (600 rpm) was used during all the trials to provide an initial estimate of crystallisation behaviour.

Further points in ternary phase diagram were measured at 4 $^{\circ}$C, 10 $^{\circ}$C and 20 $^{\circ}$C by measuring the solution concentration and solid form of the slurry with excess solids. This slurry was prepared by adding an excess of either ALA and co-crystals or excess NIC and co-crystals in 1:1 IPA-hexane and stirred at a fixed temperature for at least 24 hours to ensure the final equilibrium was reached. The slurry was filtered, and the solid form was determined by XRPD and the solution compositions were measured by HPLC.

Batch OBC Experiments on Co-crystallisation of ALA:NIC. Batch experiments were carried out in a 500 mL round-bottom jacketed glass OBC of 50 mm inner diameter. Oscillation frequency and amplitude were controlled by a linear motor. Temperature within the OBC was monitored by a Teflon® coated thermocouple, and adjusted by a *Lauda* RP845 programmable bath circulator. A mole equivalent of NIC (16 g) and filtered ALA (26.8 g) solution in isopropanol (IPA) were added to 500 ml OBC (total

working volume 480 mL). The OBC was oscillated at 1 Hz with 25 mm amplitude. At 35 °C, 240 mL of hexane was added (1:1 v/v to IPA), and the mixture was cooled from 35 to 2.5 °C in 1 hour. After filtration and drying in a vacuum oven at RT, 30.8 g of yellow co-crystals were obtained.

Continuous Co-crystallisation of ALA:NIC. The COBC was constructed from 24 m of 16 mm inner diameter jacketed glass tubes with a working volume of 4.2 L. Baffles were made of moulded glass along the length of the COBC including bends. The fluid oscillation was achieved using a PTFE bellow coupled with a linear motor and the frequency and amplitude of the oscillation were controlled via a control box. Temperature was controlled through the jacket fluid by six bath circulators and monitored by stainless steel thermocouples inserted inside the COBC along the length.

The experimental conditions listed in Table 2 were used. The solution of ALA and NIC in IPA- hexane at 40 °C was pumped into COBC by a peristaltic pump at a flow rate of 70 mL min^{-1}. The COBC temperature was reduced along the COBC length with the cooling profile displayed in Table 2. The product slurry was collected at the outlet of COBC. The continuous run was stopped after 2 - 3 hours continuous run time. Dimensionless numbers for tested operating conditions are tabulated in Table 3.

Table 2 Experimental conditions used for the continuous co-crystallisation trials

Entry	Oscillation	Cooling Rate	Flow Rate	Run Time
1	1 Hz 30 mm	2.5 °C min^{-1} from 40 °C to 15 °C,0.3 °C min^{-1} from 15 °C to 2.5 °C, hold at 2.5 °C for 11 min	70 mL min^{-1}	120 min
2	1 Hz 30 mm	2.5 °C min^{-1} from 40 °C to 15 °C, 0.45 °C min^{-1} from 15 °C to 2.5 °C, hold at 2.5 °C for 22 min	70 mL min^{-1}	120 min
3	1 Hz 30 mm	3.5 °C min^{-1} from 40 °C to 6.6 °C, 0.45 °C min^{-1} from 6.6 °C to 2.5 °C, hold at 2.5 °C for 41 min	70 mL min^{-1} with pulse seeding with 10 % seeds in 50 % IPA-hexane	155 min

Table 3 Dimensionless numbers for operating conditions used

Oscillatory Reynolds, Re_o	Net Flow Reynolds, Re_n	Strouhal, St	Velocity Ratio, Ψ
1000	80	0.09	12

Residence time distribution studies on the same COBC system[77], show that the vessel dispersion number (D/uL)[78] is less than 0.01, indicating that the system is operating close to plug flow under the operating parameters used in this study.[79]

RESULTS AND DISCUSSION

Discovery of ALA Co-crystals

Eight co-formers with either amide (-$CONH_2$), carboxylic acid (-COOH) or pyridine ring were chosen for the co-crystallisation trials based on a crystal–engineering approach. These co-formers were selected based on the prior knowledge of the potential for H-bonded supramolecular synthons to be formed between carboxylic acid (present in ALA) and complementary functionality of potential co-formers[20, 21, 35, 38] (see ESI). Three novel physical forms of ALA with NIC, ISN and trans-cinnamamide (Fig. 3). respectively were obtained from both liquid-assisted grinding and small-scale solution crystallisation. These three novel solid forms were analysed by XRPD, which confirmed the formation of a new polycrystalline phase in each case (Fig. 4). The ΔpKa values (pKa (base) - pKa (acid)) of ALA (4.70)[80] and NIC (3.40)[81, 82] and ALA and ISN (3.61)[83] are both negative suggesting these forms are co-crystals rather than salts.[84, 85]

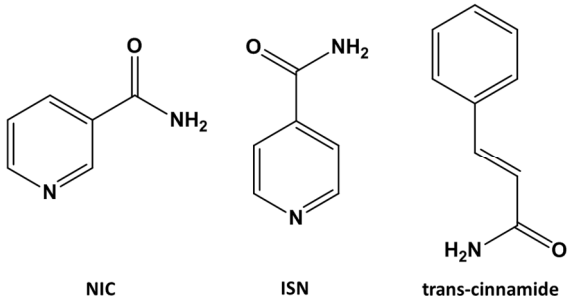

NIC ISN trans-cinnamide

Fig. 3. Chemical structures of three co-crystal formers which yielded novel co-crystals with ALA.

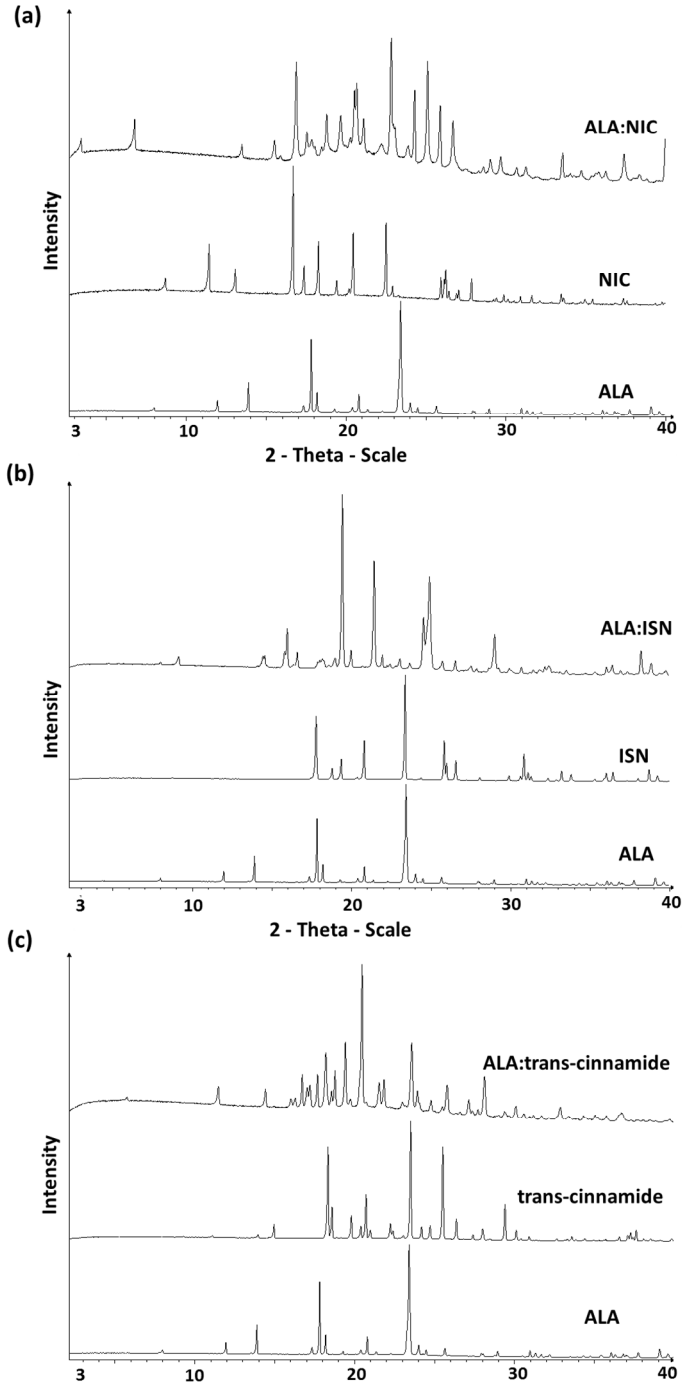

Fig. 4. Stack plots of XRPD patterns for (a) ALA, NIC and ALA:NIC co-crystals, (b) ALA, ISN and ALA:ISN co-crystals and (c) ALA, trans-cinnamide and ALA:trans-cinnamide co-crystals in the range of 2-39° 2θ.

Further supporting data including DSC and FT-IR spectra of three novel co-crystal forms are provided in the ESI. On the basis of accessible yields of co-crystals, ALA:NIC co-crystals were selected for further characterisation and scale-up study.

Crystal Structure Determination of ALA:NIC Co-crystals

The ALA:NIC co-crystal crystallises in space group $P2_1/c$ with three molecules of ALA and NIC each in the asymmetric unit. Out of three ALA molecules in the asymmetric unit, two of them are highly disordered. One of the disordered ALA molecules is disordered over two positions corresponding to the R and S configurations. The other disordered ALA molecule exists in the R configuration and is disordered over two positions. The crystal structure data obtained from SXD are reported in Table 4.

Table 4 X-ray crystallographic crystal data, data collection and refinement details of ALA:NIC collected at -150(2) °C.

Crystal Data		**Data collection**	
Chemical formula	$C_8H_{14}O_2S_2{\cdot}C_6H_6N_2O$	Diffractometer	Bruker *APEX*-II CCD
M_r	328.44	Absorption correction	Multi-scan SADABS
Crystal system, space group	Monoclinic, $P2_1/c$	T_{min}, T_{max}	0.605, 0.745
Temperature (°C)	-150 (2)	No. of measured, independent and observed [$I > 2\sigma(I)$] reflections	33254, 9068, 6027
a, b, c (Å)	26.292 (2), 5.2948 (4), 34.158 (3)	R_{int}	0.052
α, β, γ (°)	90, 90.598 (4), 90	**Refinement**	
V (Å^3)	4754.9 (6)	$R[F^2 > 2\sigma(F^2)]$, $wR(F^2)$, S	0.073, 0.215, 1.05
Z	12	No. of reflections	9068
Radiation type	Mo $K\alpha$	No. of parameters	752
μ (mm^{-1})	0.35	No. of restraints	873
Crystal size (mm)	0.15 × 0.10 × 0.03	H-atom treatment	H atoms treated by a mixture of independent and constrained refinement
		$\Delta\rangle_{max}$, $\Delta\rangle_{min}$ (e Å^{-3})	1.41, -0.40

Each ALA molecule forms two H-bonds with two NIC molecules. The hydroxyl moiety of the carboxylic acid group in ALA acts as a donor for the ring nitrogen atom of one NIC molecule with the carbonyl oxygen acting as an acceptor for the amino moiety of the amide group in second NIC (Fig. 5). ALA molecules form chains along the *c*-axis, which stack anti-parallel to each other. NIC molecules forms dimers connected by amide-amide supramolecular synthons, which further stack along *b*-axis. The columns of NIC dimers stack along *c*-axis and are present between antiparallel chains of ALA along the *a*-axis.

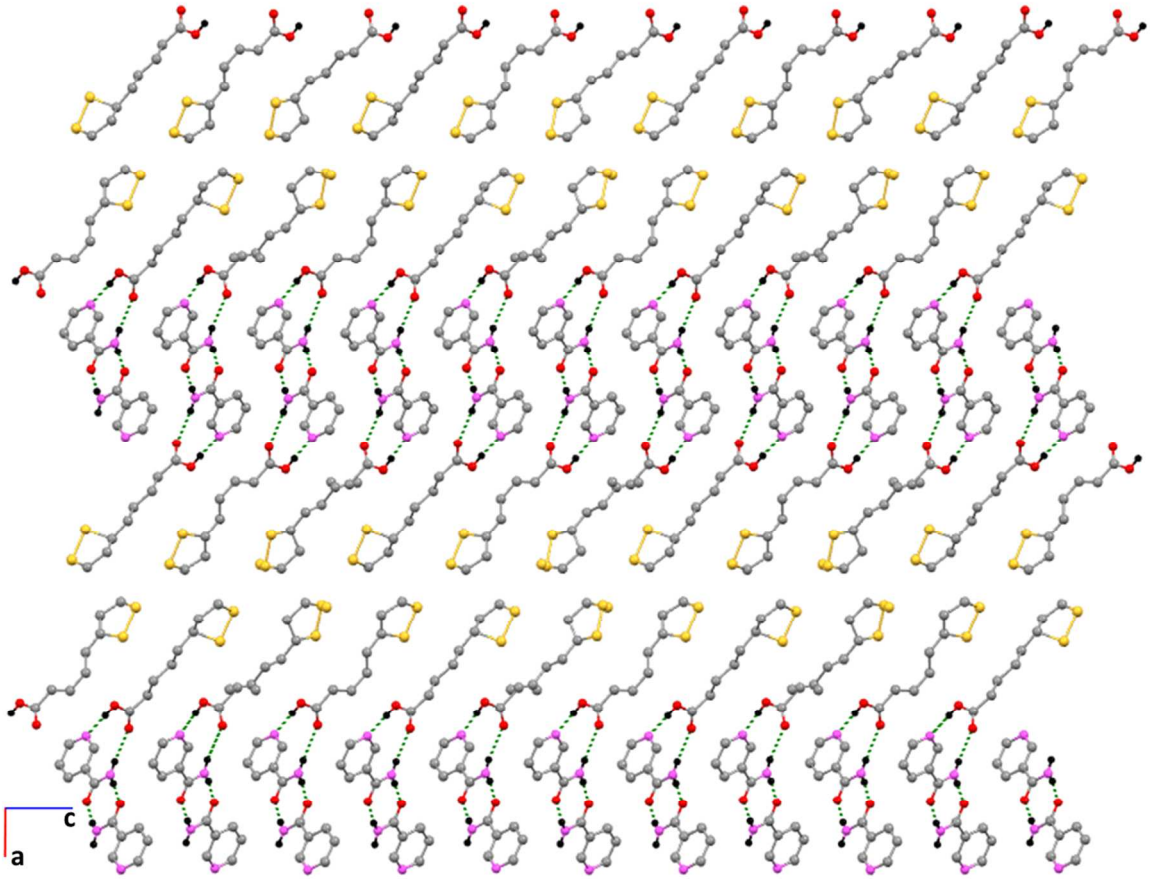

Fig. 5. The crystal packing in ALA, viewed down the *b*-axis. C, N, O, S and H atoms are shown in grey, violet, red, yellow and black, respectively. Hydrogen bonds are shown as green dotted lines. Other H atoms have been omitted for clarity.

Stability Studies of ALA:NIC Co-crystals

Thermal Analysis. ALA showed a melting endotherm with an onset temperature of 60 °C (Fig. 6a). Subsequently quench cooling to -50 °C, and heating up to 70 °C showed a very small endotherm with an onset temperature of 50 °C (Fig. 6a). No mass loss was observed in the TG curve during and after melting. The above results suggest that the ALA undergoes a transformation on heating to 65 °C. It is reported in the literature that ALA undergoes polymerisation when heated above its melting point.[8, 9]

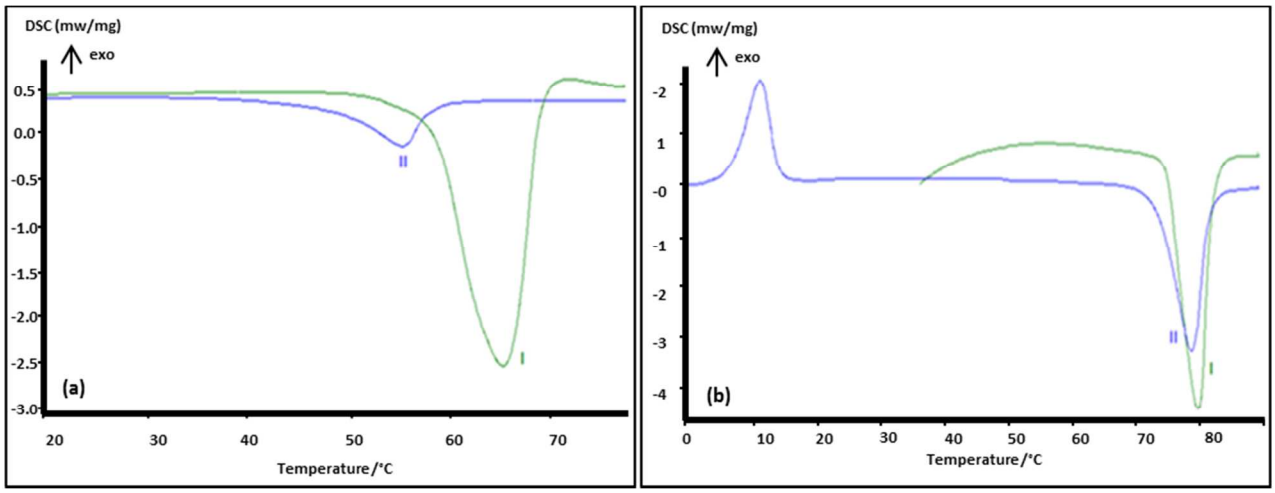

Fig. 6. DSC traces of (a) ALA with a melt endotherm (I, green colour) and heating of subsequently cooled ALA (II, blue colour) and (b) ALA: NIC co-crystals with a melt endotherm (I, green colour) and heating of subsequently cooled co-crystals (II, blue colour).

For ALA co-crystals, the DSC results were markedly different. After the ALA:NIC co-crystals melt at ~80 °C, the DSC sample was cooled to -50 °C and heated again at the same heating rate. Re-crystallisation occurred at ~8 ºC with a further melting endotherm featuring the same melting point as the starting sample (Fig. 6b). No mass loss was observed in the TG curve which further confirmed the stability of the co-crystals. Unlike starting material ALA which polymerised after the melting point, all

three novel ALA co-crystals showed no evidence of thermal decomposition/degradation in the tested temperature range (20 °C to 160 °C) (see ESI). A very recent thermal study on ALA also showed that the presence of an additive increases the thermal stability of the ALA.[86] The mechanism by which NIC improves the thermal stability of ALA is unclear, however the marked effect is not restricted to the crystalline state and is evident above the melting point of ALA and the ALA:NIC co-crystal where the components are in the liquid state.

HPLC Analysis. The results showed that ~38 % of ALA degraded after 30 minutes at 60 ºC, with 18 % of ALA remaining after 30 minutes at 80 ºC. In contrast, the co-crystals showed enhanced thermal stability as no change in ALA content was observed even after 30 minutes at 80 ºC (Table 5). The Other two co-crystals (ALA:ISN and ALA:trans-cinnamamide) also showed enhanced stability than ALA (see ESI).

Table 5 Thermal Stability of ALA and Co-crystals determined by HPLC

Crystals	Original ALA purity (%)	ALA purity after 30 minutes at 60 °C	ALA purity after 30 minutes at 80 °C
ALA	100	61.83	17.94
ALA:NIC co-crystals	100	99.73	99.58

Design of a Co-crystallisation Process

Having selected ALA:NIC as a thermally stable system for further investigation, a continuous cooling crystallisation method was investigated to scale-up the production of this co-crystal system. The first step was to select a suitable solvent system for the co-crystallisation process that will deliver good chemical and physical purity as well as yield

A solvent screen was performed using a variety of solvents to obtain initial information on relative solubilities, crystal habit and the relative kinetics of each component in the system. No polymorphism of the ALA:NIC co-crystal was observed under any of the crystallisation conditions tested in this study.

To meet with the capabilities of the COBC system available, the target was to find a suitable solvent system that could deliver the required yield (1 kg) from a cooling crystallisation with a mean residence time of less than 1 hour. It has been recommended from studies of multiple cooling crystallisation systems[87] that for an industrial cooling crystallisation process solubility in the range of 50-150 g/L at the highest temperature and > 5 g/L at the final temperature are desirable. In this work, whilst IPA was a identified as a good solvent for obtaining pure ALA:NIC co-crystals it did not display this ideal profile to deliver the required yield and so mixed IPA solvent systems were also tested. ALA:NIC co-crystals have a solubility of 229.17 g/L in IPA at 37 $^{\circ}$C. It was found that a 1:1 (v/v) IPA-hexane system gave more suitable solubility profiles (Fig. 7). In this binary solvent system, ALA has much higher solubility than the co-crystals and NIC is also more soluble than the co-crystals in the temperature range of -10 to 40 °C.

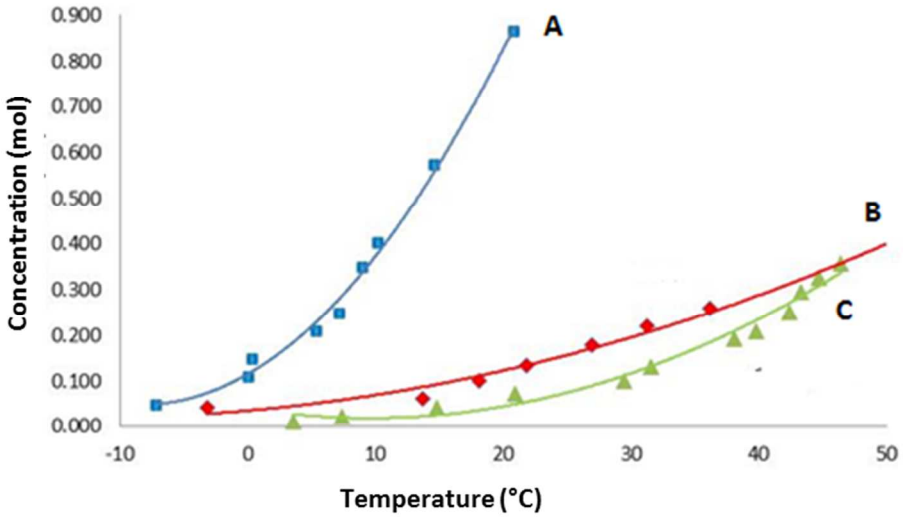

Fig. 7. Solubility curves of ALA (A), NIC (B) and ALA:NIC co-crystals (C) in 1:1 IPA-Hexane in the range -8 to 48°C.

In-situ image analysis during the solubility studies indicated the formation of spherical agglomerates. XRPD analysis confirmed the identity and physical purity of the ALA:NIC co-crystals (Fig. 8).

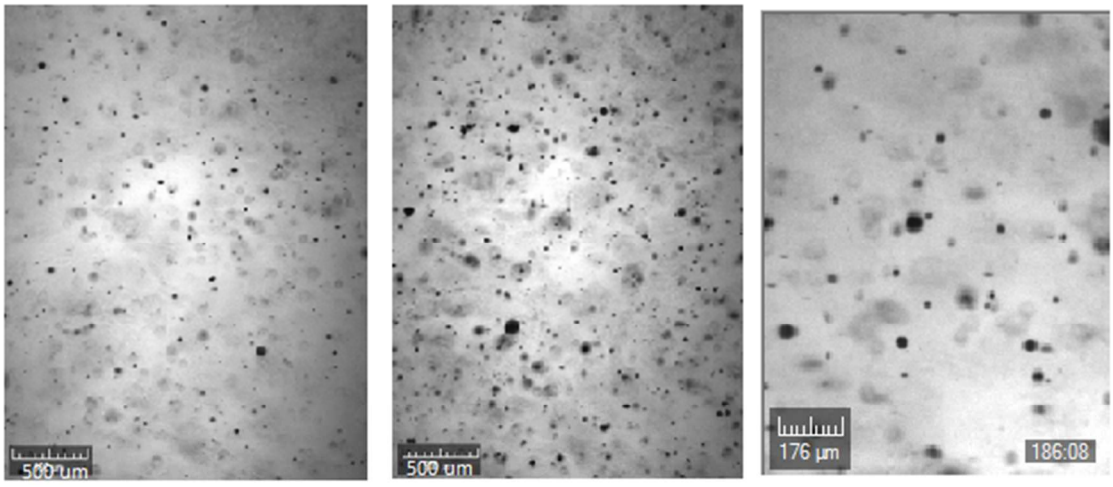

Fig. 8. Spherical agglomerates captured during in-situ image analysis of co-crystallisation in 1:1 IPA-hexane in an 8 mL stirred tank reactor.

The ternary phase diagram is of value in developing a controlled approach to co-crystal crystallisation.[88] The ternary phase diagram of ALA and NIC in the mixed solvent of IPA-hexane is shown in Fig. 9. The

eutectic points were determined based on Gibb's phase rule[89-91] and the critical region in which crystallisation of pure co-crystals occurs is shown as the region inside points A, B and C (Fig. 9).

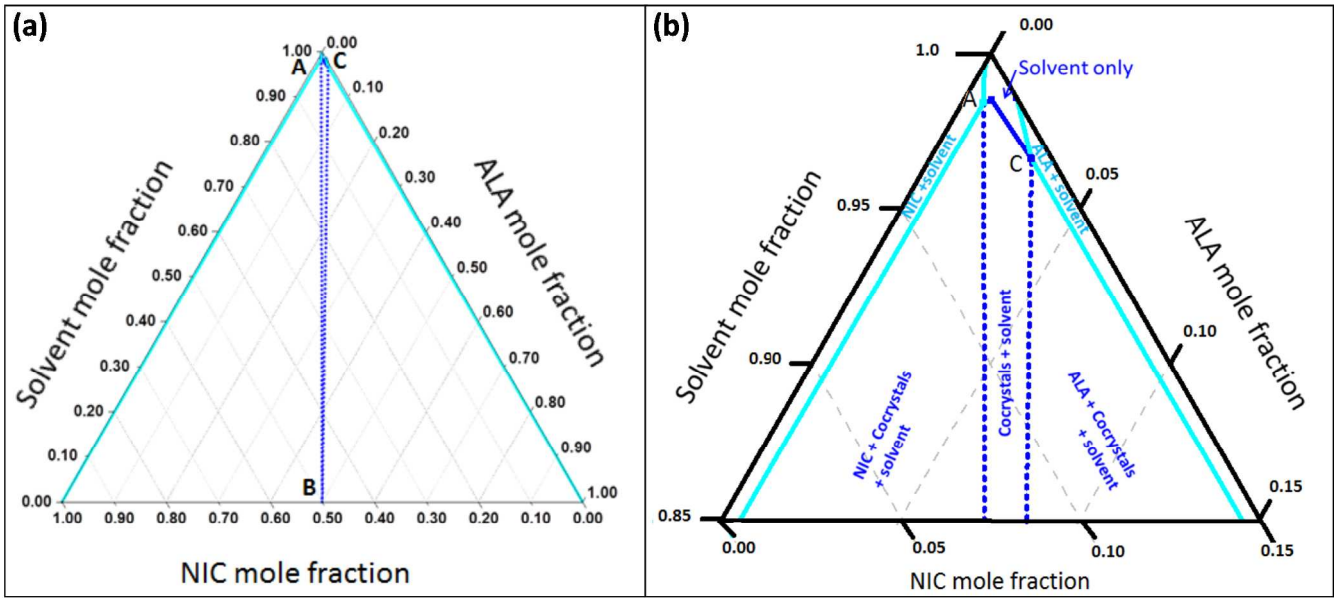

Fig. 9. (a) Ternary phase diagram of ALA, NIC in 1:1 IPA:hexane at 2 °C, (b) inset highlighting upper part of the phase diagram.

The temperature dependence of the phase diagram was also investigated to inform the process design and identify changes in the temperature dependence of the critical region (Fig. 10). The critical region becomes narrower as temperature is reduced, largely due to the significant change in ALA solubility, emphasising the importance of accurate temperature control throughout the cooling process. The starting concentrations for ALA and NIC and cooling profiles were selected to ensure the crystallisation process would be operated within the critical region optimising the purity and yield of the process.

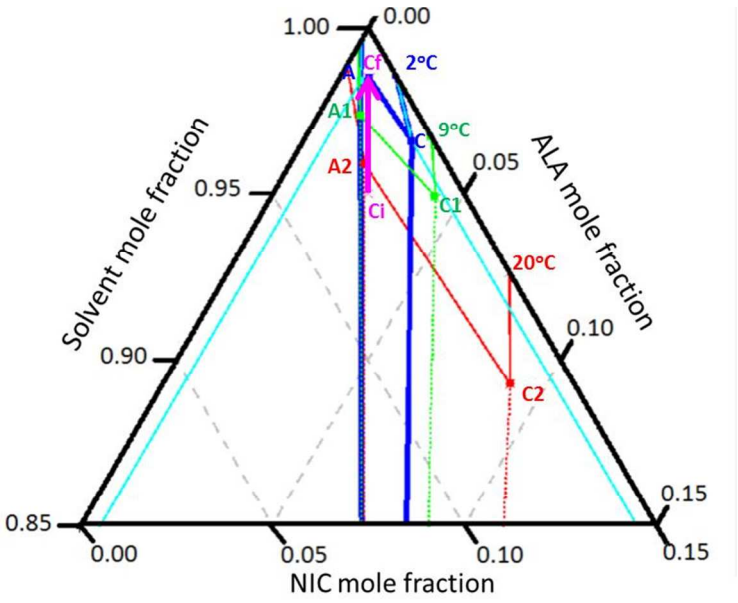

Fig. 10. Ternary phase diagram of ALA and NIC in 1:1 IPA-hexane at 2 °C, 9 °C and 20 °C. A, C and A1, C1 and A2, C2 are eutectic points at 2 °C, 9 °C and 20 °C respectively. The blue lines delineate the critical region at 2 °C, and dotted green and red lines bound the critical regions at 9 °C and 20 °C. c_i, c_f represent starting concentration and final concentration respectively.

In the next step, the co-crystallisation process of ALA and NIC in 1:1 IPA-hexane was scaled-up in a 500 mL batch OBC to identify the key parameters required for design of the continuous process. These include residence time, temperature profile, oscillation frequency and amplitude. The target was to enable complete desupersaturation of the solution within the target residence time with an acceptable yield and co-crystal purity whilst ensuring complete suspension of particles. The operation temperature range was chosen from 40 °C to 2.5 °C using equimolar starting concentrations for ALA and NIC of 0.27 M (starting concentration c_i, and final concentration c_f shown in Fig. 10). Oscillatory mixing conditions of 1 Hz and 25 mm were selected based on achieving a uniform solid suspension at the maximum solid loading. Over 30 g of pure co-crystal was obtained from two repeats (65-71 % yield). These experiments also resulted in spherical agglomerates of the co-crystal. Nucleation temperatures were higher in the batch OBC than that observed in magnetically stirred vial systems (10 °C in OBC as

compared to -2 °C in a vial). This may be due to the high shear rates and/or the scraping effect of the moving baffles used in this batch OBC compared to the magnetically stirred vials used in the small-scale experiments.[92]

Pawley type refinement of the of the lattice parameters of the ALA-NIC co-crystal obtained from SXD against the XRPD data of the samples obtained from OBC experiments showed a good fit (R_{wp} = 4.12) (see ESI), confirming the crystal structure obtained from SXD is representative of the bulk sample. FTIR and thermal analyses were also employed to confirm the purity of the co-crystals obtained from OBC experiments.

Continuous Crystallisation of ALA:NIC Co-crystals in a COBC.

The scale-up design and operation in the COBC was carried out by implementing similar oscillatory conditions as identified from the batch OBC experiments described above. To achieve reliable nucleation of the co-crystal in the cooling process, seeding was used by pumping 10 % w/w co-crystal seed suspension for 10 s at 10 °C. No further seeds were required after initiation of nucleation in the COBC. Further work is ongoing to understand the nucleation mechanisms given the operating conditions used in the COBC.

Three COBC trials were completed, running for up to 3 residence times. Solid content and particle size distributions were monitored from the outlet stream using focused beam reflectance measurement (FBRM). The product slurry had a solid content of 78 g/L equivalent to a production throughput of 330 g/hr of solid co-crystals. Fig. 11 shows the crystallisation of the ALA:NIC product at different positions in the COBC during operation.

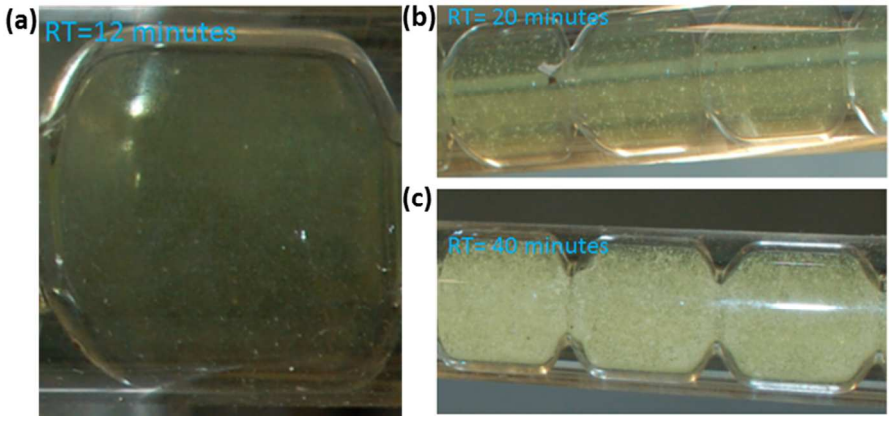

Fig. 11 Co-crystallisation in a COBC (a) at residence time (RT) = 12 minutes and shows the early stages of growth; (b) RT = 20 minutes and (c) RT = 40 minutes show the progression of crystal growth.

No signs of fouling or potential blockage were observed during these trials. SEM images of the co-crystals produced in the COBC showed that the co-crystals were spherical agglomerates comprising multiple small thin plates (Fig. 12). The co-crystals obtained from the COBC had a relatively narrow PSD as shown by SEM and FBRM (Fig. 12 and Fig. 13).

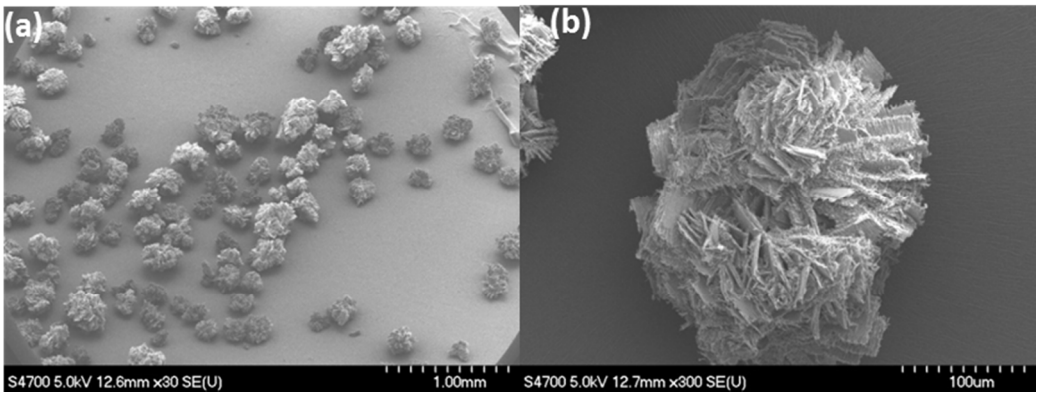

Fig. 12 SEM images of dried ALA:NIC co-crystals from the continuous trial.

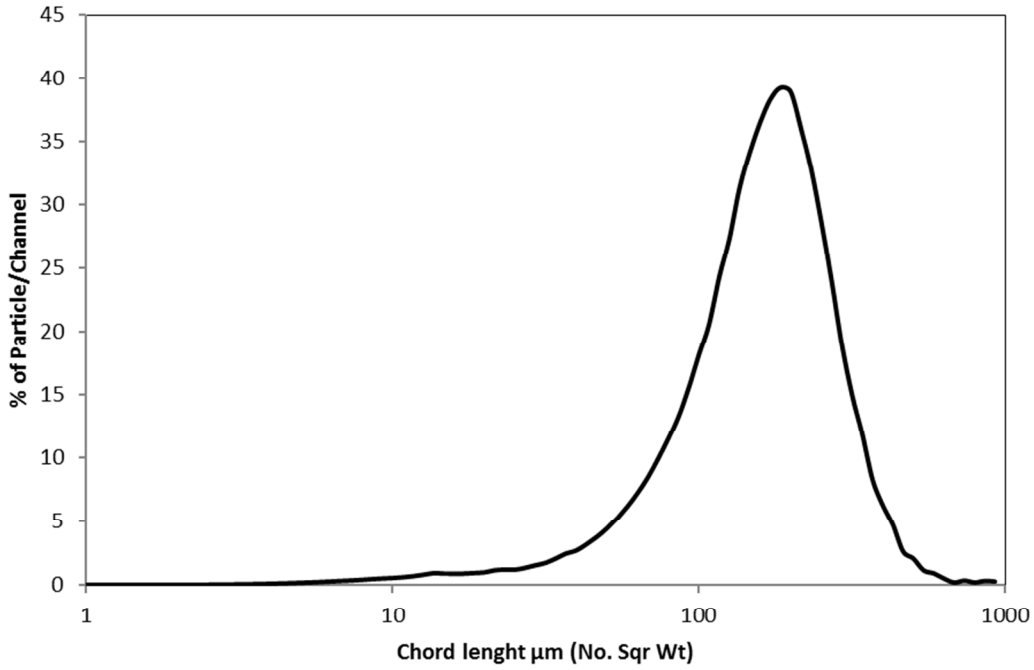

Fig. 13 Chord length distribution measured using FBRM for ALA:NIC co-crystals produced from the continuous co-crystallisation process in a COBC.

CONCLUSION

Three novel ALA co-crystals were discovered and characterised by XPRD, FTIR and thermal analysis. The crystal structure of the ALA:NIC co-crystal was determined using SXD revealing the molecular packing in this novel solid form. In addition to highlighting the specific intermolecular interactions within the lattice, the single crystal structure also provides an unambiguous means for physical identification of the co-crystal product produced using different crystallisation approaches. Here, a co-crystal product was shown to have enhanced thermal stability compared with pure ALA conferring significant advantages for production and storage of this material. Given the increased interest in the prediction, discovery and characterisation of novel functional co-crystalline materials across different application areas approaches for rapid scale-up are also of considerable interest. This study has

demonstrated the rapid translation of a novel co-crystal material from gram to kilogram scale in the laboratory using continuous crystallisation in a COBC supported by a systematic approach to process design. Agglomerated spherical co-crystals were produced continuously at a throughput of 330 g/hr of solid at a laboratory scale in good purity and narrow particle size distributions. Further work is required to detail the mechanism of nucleation following seeding and agglomeration in this process. The use of on-line PAT techniques such as IR, UV or Raman as well as imaging (e.g. PVM) are very useful tools for more advanced process understanding and control.[93, 94] The increased range of technologies becoming available for continuous crystallisation at laboratory scale provide an important approach route to accelerate the exploitation of novel materials through their consistent production at larger scales using continuous processing.

Acknowledgments. The authors thank the EPSRC Centre for Innovative Manufacturing in Continuous Manufacturing and Crystallisation (www.cmac.ac.uk) for supporting this work (EPSRC funding under grant reference: EP/I033459/1). NEBB thanks Scottish Funding Council and EPSRC SPIRIT award for funding.

Supporting information available: FTIR spectra, HPLC data, XRPD patterns, thermal analysis, and Crystallographic information file (CCDC deposition number: CCDC 982737).

References

1. G. Raddatz and H. Bisswanger, *J Biotechnol*, 1997, **58**, 89-100.
2. D. Ziegler, H. Nowak, P. Kemplert, P. Vargha and P. A. Low, *Diabetic Med*, 2004, **21**, 114-121.
3. D. Ziegler, A. Ametov, A. Barinov, P. J. Dyck, I. Gurieva, P. A. Low, U. Munzel, N. Yakhno, I. Raz, M. Novosadova, J. Maus and R. Samigullin, *Diabetes Care*, 2006, **29**, 2365-2370.

4. A. Maczurek, K. Hager, M. Kenklies, M. Sharman, R. Martins, J. Engel, D. A. Carlson and G. Munch, *Adv Drug Deliver Rev*, 2008, **60**, 1463-1470.
5. H. Yamamoto, T. Watanabe, H. Mizuno, K. Endo, J. Fukushige, T. Hosokawa, A. Kazusaka and S. Fujita, *Free Radical Res*, 2001, **34**, 69-80.
6. P. M. Ou, H. J. Tritschler and S. P. Wolff, *Biochem Pharmacol*, 1995, **50**, 123-126.
7. J. Bustamante, J. K. Lodge, L. Marcocci, H. J. Tritschler, L. Packer and B. H. Rihn, *Free Radical Bio Med*, 1998, **24**, 1023-1039.
8. R. C. Thomas and L. J. Reed, *J Am Chem Soc*, 1956, **78**, 6148-6149.
9. A. Kisanuki, Y. Kimpara, Y. Oikado, N. Kado, M. Matsumoto and K. Endo, *J Polym Sci Pol Chem*, 2010, **48**, 5247-5253.
10. R. M. Stroud and C. H. Carlisle, *Acta Crystall B-Stru*, 1972, **B 28**, 304-&.
11. F. H. Allen, *Acta Crystallogr B*, 2002, **58**, 380-388.
12. H. A. Marvin, *WO 2007/095117 A2*, 2007.
13. A. Salvi, Villani, F., Nardi, A., Dugnano, P., Angelis, B.D., *U.S. 2004/0214879 A1*, 2004.
14. D. A. Carlson, A. R. Smith, S. J. Fischer, K. L. Young and L. Packer, *Altern Med Rev*, 2007, **12**, 343-351.
15. N. Ikuta, Nakata, D. and Terao, K., *WO 2012/014746*, 2012.
16. K. Kofuji, M. Nakamura, T. Isobe, Y. Murata and S. Kawashima, *Food Chem*, 2008, **109**, 167-171.
17. H. Takahashi, Y. Bungo and K. Mikuni, *Biosci Biotech Bioch*, 2011, **75**, 633-637.
18. S. Aitipamula, R. Banerjee, A. K. Bansal, K. Biradha, M. L. Cheney, A. R. Choudhury, G. R. Desiraju, A. G. Dikundwar, R. Dubey, N. Duggirala, P. P. Ghogale, S. Ghosh, P. K. Goswami, N. R. Goud, R. R. K. R. Jetti, P. Karpinski, P. Kaushik, D. Kumar, V. Kumar, B. Moulton, A. Mukherjee, G. Mukherjee, A. S. Myerson, V. Puri, A. Ramanan, T. Rajamannar, C. M. Reddy, N. Rodriguez-Hornedo, R. D. Rogers, T. N. G. Row, P. Sanphui, N. Shan, G. Shete, A. Singh, C. Q. C. Sun, J. A. Swift, R. Thaimattam, T. S. Thakur, R. K. Thaper, S. P. Thomas, S. Tothadi, V. R. Vangala, N. Variankaval, P. Vishweshwar, D. R. Weyna and M. J. Zaworotko, *Cryst Growth Des*, 2012, **12**, 2147-2152.
19. N. Schultheiss and A. Newman, *Cryst Growth Des*, 2009, **9**, 2950-2967.
20. C. B. Aakeroy and D. J. Salmon, *Crystengcomm*, 2005, **7**, 439-448.
21. O. Almarsson and M. J. Zaworotko, *Chem Commun*, 2004, 1889-1896.
22. P. Vishweshwar, J. A. McMahon, J. A. Bis and M. J. Zaworotko, *J Pharm Sci-Us*, 2006, **95**, 499-516.

23. H. G. Brittain, *Cryst Growth Des*, 2012, **12**, 5823-5832.
24. S. J. Bethune, N. Schultheiss and J. O. Henck, *Cryst Growth Des*, 2011, **11**, 2817-2823.
25. P. Sanphui, N. R. Goud, U. B. R. Khandavilli and A. Nangia, *Cryst Growth Des*, 2011, **11**, 4135-4145.
26. D. I. A. Millar, H. E. Maynard-Casely, D. R. Allan, A. S. Cumming, A. R. Lennie, A. J. Mackay, I. D. H. Oswald, C. C. Tang and C. R. Pulham, *Crystengcomm*, 2012, **14**, 3742-3749.
27. O. Bolton, L. R. Simke, P. F. Pagoria and A. J. Matzger, *Cryst Growth Des*, 2012, **12**, 4311-4314.
28. E. Nauha and M. Nissinen, *J Mol Struct*, 2011, **1006**, 566-569.
29. A. V. Trask, *Mol Pharm*, 2007, **4**, 301-309.
30. E. K. Starostin, A. V. Lalov, A. V. Ignatenko and G. I. Nikishin, *Mendeleev Commun*, 2008, **18**, 123-125.
31. W. M. Fischer and A. Taurinsch, *Ber Dtsch Chem Ges*, 1931, **64**, 236-239.
32. J. G. I. Amos, J. M.; Pasini, C. E.; Reutzel, S. M., *U.S. 1999/6001996*, 1999.
33. P. Billot, Hosek, P. and Perrin, M., *Org Process Res Dev*, 2013, **17**, 505-511.
34. B. N. Roy, G. P. Singh, D. Srivastava, H. S. Jadhav, M. B. Saini and U. P. Aher, *Org Process Res Dev*, 2009, **13**, 450-455.
35. T. Friscic and W. Jones, *Faraday Discuss*, 2007, **136**, 167-178.
36. N. Blagden, M. de Matas, P. T. Gavan and P. York, *Adv Drug Deliver Rev*, 2007, **59**, 617-630.
37. P. Vishweshwar, J. A. McMahon, M. L. Peterson, M. B. Hickey, T. R. Shattock and M. J. Zaworotko, *Chem Commun*, 2005, 4601-4603.
38. M. C. Etter, *Accounts Chem Res*, 1990, **23**, 120-126.
39. T. Friscic, W. Jones and W. D. Samuel, *Abstr Pap Am Chem S*, 2007, **233**.
40. M. Habgood and S. L. Price, *Cryst Growth Des*, 2010, **10**, 3263-3272.
41. J. F. Remenar, S. L. Morissette, M. L. Peterson, B. Moulton, J. M. MacPhee, H. R. Guzman and O. Almarsson, *J Am Chem Soc*, 2003, **125**, 8456-8457.
42. S. J. Nehm, B. Rodriguez-Spong and N. Rodriguez-Hornedo, *Cryst Growth Des*, 2006, **6**, 592-600.
43. S. L. Childs, L. J. Chyall, J. T. Dunlap, V. N. Smolenskaya, B. C. Stahly and G. P. Stahly, *J Am Chem Soc*, 2004, **126**, 13335-13342.
44. R. D. B. Walsh, M. W. Bradner, S. Fleischman, L. A. Morales, B. Moulton, N. Rodriguez-Hornedo and M. J. Zaworotko, *Chem Commun*, 2003, 186-187.

45. G. G. Z. Zhang, R. F. Henry, T. B. Borchardt and X. C. Lou, *J Pharm Sci-Us*, 2007, **96**, 990-995.
46. D. Braga and F. Grepioni, *Angew Chem Int Edit*, 2004, **43**, 4002-4011.
47. R. Kuroda, Y. Imai and N. Tajima, *Chem Commun*, 2002, 2848-2849.
48. T. Friscic, A. V. Trask, W. Jones and W. D. S. Motherwell, *Angew Chem Int Edit*, 2006, **45**, 7546-7550.
49. D. J. Berry, C. C. Seaton, W. Clegg, R. W. Harrington, S. J. Coles, P. N. Horton, M. B. Hursthouse, R. Storey, W. Jones, T. Friscic and N. Blagden, *Cryst Growth Des*, 2008, **8**, 1697-1712.
50. C. Medina, D. Daurio, K. Nagapudi and F. Alvarez-Nunez, *J Pharm Sci-Us*, 2010, **99**, 1693-1696.
51. A. L. Kelly, T. Gough, R. S. Dhumal, S. A. Halsey and A. Paradkar, *Int J Pharmaceut*, 2012, **426**, 15-20.
52. R. S. Dhumal, A. L. Kelly, P. York, P. D. Coates and A. Paradkar, *Pharm Res-Dordr*, 2010, **27**, 2725-2733.
53. A. Y. Sheikh, S. A. Rahim, R. B. Hammond and K. J. Roberts, *Crystengcomm*, 2009, **11**, 501-509.
54. M. B. Hickey, M. L. Peterson, L. A. Scoppettuolo, S. L. Morrisette, A. Vetter, H. Guzman, J. F. Remenar, Z. Zhang, M. D. Tawa, S. Haley, M. J. Zaworotko and O. Almarsson, *Eur J Pharm Biopharm*, 2007, **67**, 112-119.
55. Z. Q. Yu, P. S. Chow and R. B. H. Tan, *Cryst Growth Des*, 2010, **10**, 2382-2387.
56. D. H. Leung, S. Lohani, R. G. Ball, N. Canfield, Y. L. Wang, T. Rhodes and A. Bak, *Cryst Growth Des*, 2012, **12**, 1254-1262.
57. J. W. Mullin, *Crystallization*, 4th edn., Butterworth-Heinemann, Oxford, 2001.
58. C. Jimenez-Gonzalez, P. Poechlauer, Q. B. Broxterman, B. S. Yang, D. A. Ende, J. Baird, C. Bertsch, R. E. Hannah, P. Dell'Orco, H. Noorrnan, S. Yee, R. Reintjens, A. Wells, V. Massonneau and J. Manley, *Org Process Res Dev*, 2011, **15**, 900-911.
59. P. Poechlauer, J. Manley, R. Broxterman, B. Gregertsen and M. Ridemark, *Org Process Res Dev*, 2012, **16**, 1586-1590.
60. N. G. Anderson, *Org Process Res Dev*, 2012, **16**, 852-869.
61. C. Vervaet and J. P. Remon, *Chem Eng Sci*, 2005, **60**, 3949-3957.

62. S. Mascia, P. L. Heider, H. Zhang, R. Lakerveld, B. Benyahia, P. I. Barton, R. D. Braatz, C. L. Cooney, J. M. B. Evans, T. F. Jamison, K. F. Jensen, A. S. Myerson and B. L. Trout, *Angew. Chem. Int. Edit.*, 2013, **52**, 12359-12363.
63. S. Lawton, G. Steele, P. Shering, L. H. Zhao, I. Laird and X. W. Ni, *Org Process Res Dev*, 2009, **13**, 1357-1363.
64. P. Stonestreet and P. M. J. Van der Veeken, *Chem Eng Res Des*, 1999, **77**, 671-684.
65. X. Ni, M. R. Mackley, A. P. Harvey, P. Stonestreet, M. H. I. Baird and N. V. R. Rao, *Chem Eng Res Des*, 2003, **81**, 373-383.
66. A. P. Harvey, M. R. Mackley and T. Seliger, *J Chem Techbol Biot*, 2003, **78**, 338-341.
67. A. P. Harvey, M. R. Mackley and P. Stonestreet, *Ind Eng Chem Res*, 2001, **40**, 5371-5377.
68. M. Mackay, M. M. R. and W. Y., *Trans I.Chem.E.*, 1991, **69A,** , 506-513
69. M. R. Mackley, S. K.B. and W. N.P., *Trans I.Chem.E.*, 1993, **71A** 649-656.
70. X. Ni, H. Jian and A. Fitch, *Chem Eng Res Des*, 2003, **81**, 842-853.
71. H. Jian and X. Ni, *Chem Eng Res Des*, 2005, **83**, 1163-1170.
72. X. Ni, Y. S. De Gélicourt, M. H. I. Baird and N. V. R. Rao, *Can J Chem Eng*, 2001, **79**, 444-448.
73. K. B. Smith and M. R. Mackley, *Chem Eng Res Des*, 2006, **84**, 1001-1011.
74. *Bruker AXS Inc, APEXII User Manual, Analytical X-ray Systems, 5465 East Cheryl Parkway, Madison, WI 53711-5373*, 2005.
75. G. Sheldrick, *Acta Crystallogra A*, 2008, **64**, 112-122.
76. L. J. Farrugia, *J Appl Cryst*, 1999, **32**, 837-838.
77. N. E. B. Briggs, J. Sefcik and A. J. Florence, Residence time distribution and heat transfer performance in continous oscillatroy baffled crytsalliser, Article in preparation.
78. M. Zheng and M. Mackley, *Chem Eng Sci*, 2008, **63**, 1788-1799.
79. O. Levenspiel, *Chemical Reaction Engineering*, 3rd edn., Wiley, New York 1999.
80. L. J. Reed, B. G. Debusk, I. C. Gunsalus and G. H. F. Schnakenberg, *J Am Chem Soc*, 1951, **73**, 5920-5920.
81. A. Guven, *Int. J. Mol. Sci.*, 2005, **6**, 257-275.
82. E. B. Hughes, H. H. G. Jellinek and B. A. Ambrose, *J. Phys. Colloid Chem.*, 1949, **53**, 410-414.
83. H. H. G. Jellinek and J. R. Urwin, *J. Phys. Chem.*, 1954, **58**, 168-173.
84. S. L. Childs, G. P. Stahly and A. Park, *Mol Pharm*, 2007, **4**, 323-338.
85. B. R. Bhogala, S. Basavoju and A. Nangia, *Crystengcomm*, 2005, **7**, 551-562.
86. J. Zhang, L. Dang and H. Wei, *J. Therm Anal Calorim*, 2013, **111**, 2063-2068.

87. F. L. Muller, M. Fielding and S. Black, *Org Process Res Dev*, 2009, **13**, 1315-1321.
88. R. A. Chiarella, R. J. Davey and M. L. Peterson, *Cryst. Growth Des.*, 2007, **7**, 1223-1226.
89. J. W. Gibbs, *The Scientific papers of J Willard Gibbs vol. 1 Thermodynamics*, Dover Publications Inc., New York, 1961.
90. S. Zhang and A. C. Rasmuson, *Crystengcomm*, 2012, **14**, 4644-4655.
91. A. Ainouz, J. R. Authelin, P. Billot and H. Lieberman, *Int J Pharmaceut*, 2009, **374**, 82-89.
92. C. J. Callahan and X.-W. Ni, *Cryst Growth Des*, 2012, **12**, 2525-2532.
93. Z. K. Nagy, G. Fevotte, H. Kramer and L. L. Simon, *Chem Eng Res Des*, 2013, **91**, 1903-1922.
94. W. Chew and P. Sharratt, *Anal Methods*, 2010, **2**, 1412-1438.

Table of Content

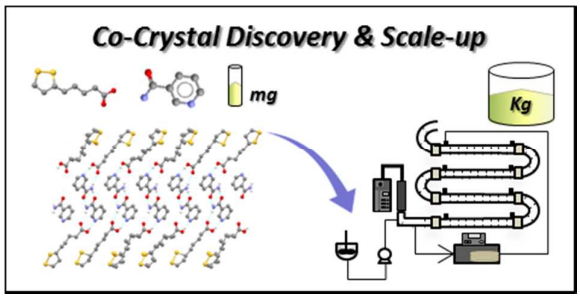

Discovery, characterisation and scale-up of novel α-lipoic acid co-crystals using continuous crystallisation in a COBC is demonstrated.